

Anomalous phase relations of quantum size effects in ultrathin Pb films on Si(111)Jisun Kim,¹ Chendong Zhang,^{1,2} Jungdae Kim,^{1,*} Hongjun Gao,² Mei-Yin Chou,^{3,4} and Chih-Kang Shih^{1,†}¹*Department of Physics, The University of Texas, Austin, TX 78712, USA*²*Institute of Physics, Chinese Academy of Sciences, Beijing, China*³*School of Physics, Georgia Institute of Technology, Atlanta, GA 30332-0430, USA*⁴*Institute of Atomic and Molecular Sciences, Academia Sinica, Taipei 10617, Taiwan*

(Received 7 October 2011; revised manuscript received 12 December 2012; published 26 June 2013)

Quantum oscillations of work function and film stability as a function of the film thickness in Pb thin films on Si(111) are measured directly using scanning tunneling microscopy and spectroscopy in order to determine their phase relationship. The comparison of the phase relationship in quantum oscillations (surface energy vs work function) reveals a complete surprise: In contrast to a theoretically predicted quarter wavelength phase shift in the phase relationship, we found that their quantum oscillations have identical phase for this particular system. A conjecture to resolve this contradiction is also provided.

DOI: [10.1103/PhysRevB.87.245432](https://doi.org/10.1103/PhysRevB.87.245432)

PACS number(s): 73.21.Fg, 73.20.At, 68.35.Md, 73.30.+y

I. INTRODUCTION

Investigations of quantum size effects in ultrathin metallic films have recently gained a tremendous amount of interest. These interests are largely driven by the advancement of atomic-scale control in epitaxial growth of metallic thin films, thus making it possible to access this strongly confined regime. These investigations have also led to discoveries of many intriguing physical phenomena manifested by the quantum size effect. For example, it has been discovered that quantum confinement can profoundly influence the thermodynamic stability of epitaxial thin films—the so-called “electronic growth” or “quantum growth” phenomena.^{1–13} Another example is the quantum size effect on the work function of metallic thin films, a phenomenon predicted four decades ago,¹⁴ but addressed experimentally only very recently.^{15–19} Among all material systems, Pb on Si(111) has been the most intensively investigated one. This is due to the nearly half-integer phase matching between the Fermi wavelength and the lattice spacing along [111], leading to bilayer quantum oscillation phenomena for many physical properties, which have been observed experimentally. Several *ab initio* calculations also suggest such quantum oscillations for additional physical properties such as the surface energy (E_s) and the work function (W).^{20,21}

One very interesting feature consistently reproduced from these theoretical calculations is the phase relationship in the quantum oscillations of the surface energy and the work function as a function of the film thickness (E_s vs L and W vs L): They are not in phase.^{20–22} Within a quantum beat period of about 9 monolayers (ML), these two quantities (E_s and W) are roughly in phase in half of the period and out-of-phase in the other half. A recent model calculation²² further elucidated this phase relationship as a consequence of a quarter wavelength phase shift with respect to a continuous variable of L . Experimentally, photoemission studies of the Ag/Fe(100) system provide some supporting evidences for this $\pi/2$ phase-shift relationship, where the surface energy²³ and the work function¹⁵ were measured separately, and then their phase relationship was demonstrated.²² In Ref. 22, it was pointed out that a Fermi level crossing happens at every 5.7 ML, and the expected quarter wavelength offset, 1.4 ML (5.7 ML/4), was observed between the surface energy and the work

function oscillation in Ag/Fe(100). However, due to the long period (5.7 ML), the beating effect was not apparent in this system, and only two quantum oscillation periods (12 ML \sim 5.7 ML \times 2) could be probed experimentally. Interestingly, such an experiment, which directly focused on the determination of the phase relationship, had not been carried out for Pb on Si(111)—the most widely investigated quantum thin film system. Using scanning tunneling microscopy and spectroscopy (STM/S), we report the first direct experimental determination of the phase relationship between quantum oscillations of E_s vs L and W vs L in Pb on Si(111). To our surprise, such a $\pi/2$ phase-shift relationship is completely absent in Pb on Si(111). In fact, these two quantities (E_s vs L and W vs L) are in phase within a large layer thickness range (from 8 to 24 ML), spanning over eight oscillation periods (\sim 16 ML = 2 ML \times 8). We further propose a model to account for this total absence of phase shift.

II. EXPERIMENTAL METHOD

All experiments were carried out in a home-built, low-temperature, ultrahigh vacuum (UHV) chamber of a scanning tunneling microscope at a base pressure $< 1.0 \times 10^{-10}$ torr. STM measurements were carried out either at 78 K or 6.5 K with the same result. Si(111) wafers (n-doped with a resistivity of 0.022–0.06 Ωcm) with 1.1° miscut toward $[\bar{1}\bar{1}2]$ were utilized. Pb was deposited on Si(111)- 7×7 at room temperature from a thermal evaporator with a typical growth rate of 0.4 ML/min. The room-temperature growth results in a Pb mesa structure with a flat-top geometry.^{24–27} Additional submonolayer Pb was deposited on Pb mesas to determine the quantum stability at a sample temperature of 95 K and further annealed at 145–255 K. The differential conductance images (dI/dV) were acquired by using a lock-in amplifier with $V_{\text{mod}} = 16$ mV and $f_{\text{mod}} = 1.4$ –1.6 kHz. Similarly, the derivative of the tunneling current with respect to tip-to-sample distance (dI/dz) was acquired by using a lock-in amplifier with $z_{\text{mod}} = 0.01$ nm and $f_{\text{mod}} = 1.4$ kHz. From the measured quantity dI/dz , the tunneling decay constant κ was calculated as $\kappa = -(dI/dz)/2I_o$, where I_o is the set current. WSxM

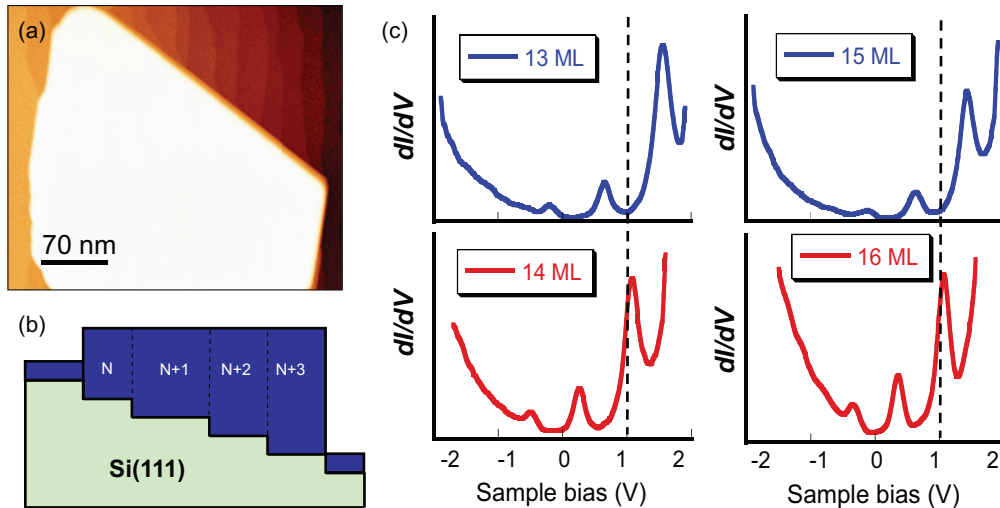


FIG. 1. (Color online) (a) Flat-top Pb mesa grown on Si(111). (b) Schematic of a mesa structure. Due to the underlying Si steps, this structure has a series of consecutive thicknesses including quantum stable and unstable thicknesses. (c) Tunneling spectra (dI/dV) of thin Pb quantum films at different thicknesses.

software was among the tools used for image preparation and analysis.²⁸

III. PHASE RELATIONSHIP IN SURFACE ENERGY AND WORK FUNCTION OSCILLATIONS

There already exists a vast body of literature investigating the quantum stability (i.e., E_s vs L) in the Pb/Si system. For example, by investigating the height distribution of 2D Pb islands either using STM^{5–7,29} or using x-ray scattering,^{30,31} probability distribution can be associated with the quantum oscillations of the film stability. A different approach uses STM to investigate the extended thin film growth as a function of layer thickness, from which only the “quantum stable” thicknesses are observed.⁹ Here, we use yet another approach to determine the quantum stability based on homoepitaxial growth of additional 2D islands on flat-top mesas, as described below. This approach has additional advantages of allowing us to simultaneously correlate quantum well state (QWS) locations, E_s , and W as a function of the thickness, thus enabling unambiguous determination of the phase relationship of E_s vs W . Figure 1(a) shows a STM image of a typical mesa structure before an additional Pb deposition. On such a mesa, QWS and W as a function of layer thickness can be simultaneously determined, and their relationship can be directly correlated. As shown in Fig. 1(b), due to the underlying Si steps, a flat-top mesa structure has a series of consecutive thicknesses, including quantum stable and unstable thicknesses; this makes it a perfect template to investigate E_s and W as a function of thickness. A typical mesa structure in the current study has a range of thicknesses from 8 ML to 24 ML. Therefore, the QWS determination of each thickness is rather straightforward from scanning tunneling spectra, as shown in Fig. 1(c). Distinctive QWS peaks can be measured on every layer of the mesa, and its thickness can be directly assigned from the topographic height of such layers. We should mention that our layer thickness is referenced to the wetting layer (WL). This reference is primary historical, as in early studies there were disagreements

regarding the thickness of the WL. Currently, it is generally agreed that the WL is about 1 ML. In some literatures, this WL is included in their determination of the thickness.

As a consequence of such a distinctive layer dependence of the QWS positions, the differential conductance image (dI/dV) acquired at a sample bias of $V_{\text{sample}} = 1$ V reveals a clear contrast between different layers within the same mesa, as shown in Fig. 2(a), which is mapped simultaneously with Fig. 1(a). The positions corresponding to 1 V in the dI/dV spectra [Fig. 1(c)] are labeled with a dashed line. The

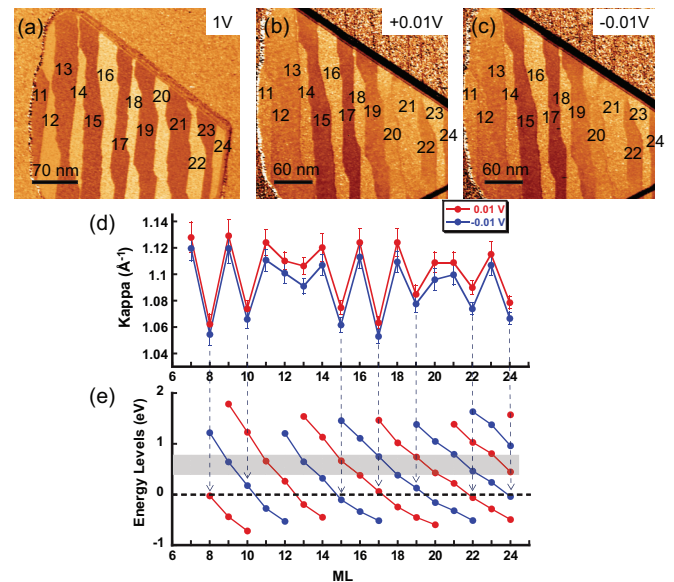


FIG. 2. (Color online) (a) dI/dV image of the same mesa as Fig. 1(a), acquired at $V_{\text{sample}} = 1$ V and tunneling set current $I_o = 70$ pA. (b, c) The corresponding dI/dz images acquired at ± 0.01 V respectively. (d) The tunneling decay constant, κ , as a function of thickness, acquired at the very low sample biases. (e) The QWS locations as a function of thickness. Note that all thicknesses are referenced to the WL.

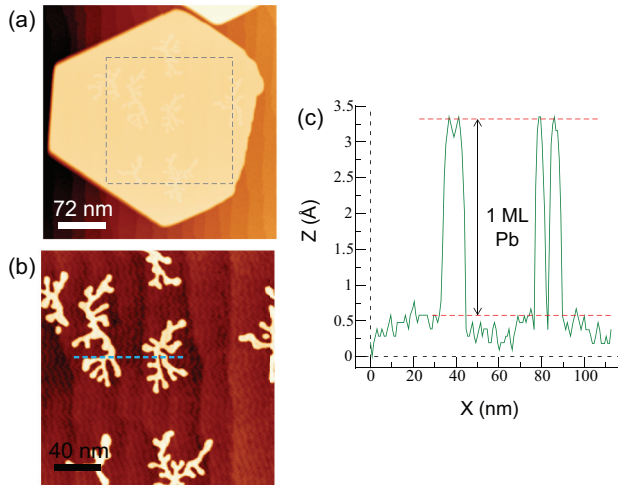


FIG. 3. (Color online) (a) Topographic image of a mesa showing additional fractal-shaped islands after 0.1 ML Pb deposition. (b) Magnified image of the area marked in (a) with a square. (c) Line profile crossing two fractal-shaped islands in the location indicated by the dashed line in (b).

determination of work function using STM, on the other hand, is not trivial. In STM, the tunneling current (I) is related to the tunneling decay constant (κ): $I \propto e^{-2\kappa z}$, and κ is related to the derivative of the tunneling current with respect to tip-to-sample distance (dI/dz): $\kappa \equiv -d \ln I / 2dz$. Earlier attempts to determine work function oscillation using STM by measuring κ yielded incorrect results. Recently, Kim *et al.*¹⁹ revealed that correct work function variations in Pb quantum films can be measured using STM by measuring κ only if probing states near the Fermi energy. Here, we adopted the same approach: We measured dI/dz at very low sample bias to acquire κ correctly reflecting work function oscillation. Figures 2(b) and 2(c) shows spatial mappings of dI/dz acquired at ± 10 mV, respectively, exhibiting the work function contrast at different thicknesses. The measured decay constant as a function of thickness is plotted in Fig. 2(d), accompanied by the measured QWS locations shown in Fig. 2(e). As theoretically predicted in Ref. 14 and observed by Kim *et al.*,¹⁹ strong suppression of the work function occurs when the QWS crosses the Fermi energy.

To reveal the modulation of surface energy due to the quantum confinement effect, we utilize the phenomena of selective homoepitaxy of additional 2D islands onto flat-top mesas that contain a large range of thicknesses, including both stable and unstable thicknesses as explained earlier. When an additional 0.1 ML of Pb is deposited on typical mesas at low temperature (95 K) and further annealed to 145 K for a few minutes, fractal-shaped islands are observed on the mesas [Fig. 3(a)]. This fractal shape is clearly seen in Fig. 3(b), and it is a characteristic of diffusion-limited aggregation (DLA),^{32,33} which results from the low mobility of deposited Pb atoms at the experimental growth temperature. All fractal islands are 1 ML high, as shown in the line profile [Fig. 3(c)]. After the initial growth, the same sample is annealed to higher temperatures without further deposition of Pb. The evolution of the island's shape is shown in Fig. 4(a)–4(c). Initially, islands preserve their fractal shapes up to the annealing temperature

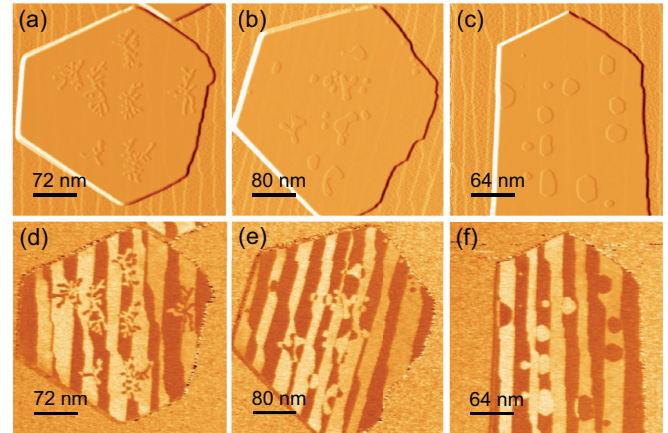


FIG. 4. (Color online) (a–c) Topographic images (light shaded for better contrast) showing the distribution of Pb islands grown on different mesas. Initially 0.1 ML of Pb is deposited, and the sample is further annealed to (a) 145 K, (b) 225 K, and (c) 255 K. (d–f) Differential conductance images (dI/dV) taken simultaneously at the sample bias of $V_{\text{sample}} = 1$ V.

of 195 K, but they start to change at a higher annealing temperature into more rounded shapes with fewer branches at 225 K [Fig. 4(b)] and an elongated circular shape with no branches at 255 K [Fig. 4(c)]. While the initial fractal-shaped islands span across a region containing two to three different thicknesses, the sign of the correlation is visible: Islands are preferentially centered around certain thicknesses, as shown in Fig. 4(d). With further annealing, this preference evolves into a total confinement of individual 2D islands completely within certain thicknesses, as shown in Fig. 4(f). As discussed below, this phenomenon is a direct manifestation of the thickness-dependent surface energy.

The formation of the flat-top mesa structure is a result of an energetic competition between the surface energy due to vertical quantum confinement and the step energy.^{25,27} Initially, flat-top geometry is established in order to avoid the high energy cost of forming multiple steps, and, as a consequence, quantum stable and unstable thicknesses coexist in one mesa. When additional Pb atoms are deposited on the surface, the formation of 2D islands inevitably results in step edges at the island boundaries, regardless of whether they are on top of the stable or unstable thicknesses. The remaining energy term is then the surface energy contribution due to the vertical confinement of electrons. Consequently, 2D islands are preferentially formed on the quantum unstable thicknesses, thereby converting the local region into a quantum stable thickness. Therefore, by monitoring the evolution of Pb islands on a mesa, quantum “unstable” (high surface energy) thicknesses are successfully assigned.

Figure 5(a) shows the island distribution (percentage coverage) as a function of thickness at each annealing temperature. Each data point is based on a statistical analysis of many mesas with an average area of around 100,000 nm² each. Layers of thicknesses ranging from 9 to 19 ML are observed on almost all mesas in our study. The sampled size of each layer is at least 18,000 nm² or larger. In fact, 20 ML is observed on fewer mesas (2–3 mesas) with a sampling size of more than 12,000 nm². Some thicknesses were observed only on

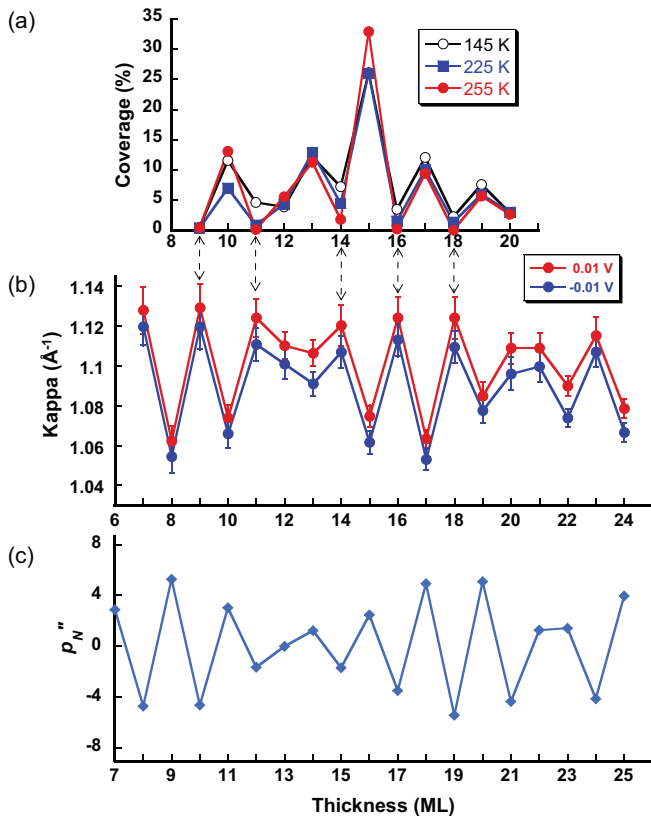


FIG. 5. (Color online) (a) Quantitative analysis of the Pb island coverage (%) as a function of thickness (ML) for each annealing temperature. (b) The corresponding work function as a function of thickness. (c) The second derivative in probability distribution function (p_N'') of Pb islands on Si(111) as a function of thickness (results taken from Ref. 31). For a direct comparison to (a) and (b), one needs to subtract 1 ML (wetting layer) from these Pb thicknesses.

one mesa among all studied mesas, but these were excluded from Fig. 5(a) due to too small sampling size. As one can observe, even at the lowest annealing temperature of 145 K, the bilayer oscillation of island distribution is quite obvious, and its tendency gets stronger with further annealing. At 255 K, odd layers before 12 ML and even layers after 12 ML show almost no island distribution, which indicates that these layers are quantum stable, making them consistent with previously reported results.⁹ Thus, Fig. 5(a) effectively represents E_s vs L , where a high peak corresponds to unstable thicknesses, i.e., high surface energy. When compared to the experimentally measured work function as a function of thickness [Fig. 5(b)], much to our surprise, E_s vs L is perfectly in phase with W vs L : All of the low work function locations correspond to the locations of unstable thicknesses (high surface energy), and vice versa. We have also compared the result of E_s vs L with those results reported in existing literature using different experimental methods and found a consistent result for E_s vs L in all cases.^{9,30,31} For example, Fig. 5(c) shows the result of the second derivative in the probability distribution function based on an x-ray scattering investigation of Pb islands on Si(111) from Ref. 31 (in their result, the thickness includes 1 ML of wetting layer). In comparison with our work function determination, except for one data point at 21 ML, the

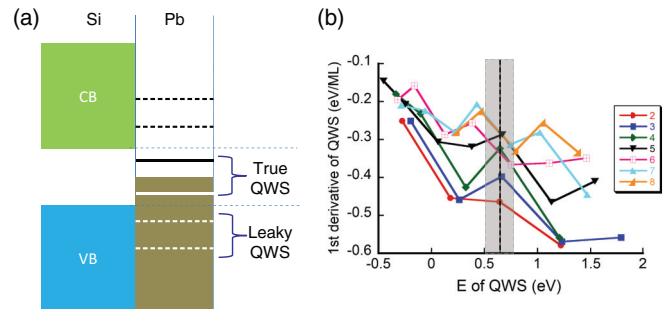


FIG. 6. (Color online) (a) A schematic showing QWS of thin Pb films with band edges of Si substrate. Only QWSs formed within a Si band gap are truly confined. (b) First derivative of QWS energy as a function of QWS energy. Kinks are present near the conduction band edge. Numbers in the legend indicate n th (counted from the left side) QWS branches shown in Fig. 2(e).

anticipated phase shift is totally absent: The locations of the low work function coincide with the locations of high surface energy. Thus, the experimental evidence for this lack of phase shift between W vs L and E_s vs L in the Pb/Si(111) system is overwhelming.

Miller *et al.*²² suggested a general phase rule that the oscillations in the surface energy as a function of film thickness lead the oscillations in the work function by quarter of a period. The original derivation was based on the assumptions that the energy dispersion is isotropic and parabolic and that the QWS energy is an analytic function of film thickness that is treated as a continuous variable. Using the corresponding parameters for Pb films, one finds that the oscillation maxima in the surface energy lead the oscillation maxima in the work function by only about 0.18 ML. This phase difference turns out to be quite significant in the beat pattern of the envelope function associated with the data points at integer layers, since the envelope function has a much larger period than the even-odd oscillation. Thus, it should result in quarter wavelength offset between two envelope functions: The antinodes of the surface energy coincide with the nodes of the work function, but this offset is totally absent as shown in Fig. 5.

IV. CONJECTURE TO SOLVE THE ANOMALY

What could be responsible for the total absence of this quarter phase difference between W vs L and E_s vs L in Pb/Si(111)? Here we propose a conjecture involving the roles played by the band edges of the underlying substrate. In our system, Pb films are on a Si substrate with the top of the valence bands at about $E_0 = -0.5$ eV. Only QWSs within the band gap of the substrate are truly confined [Fig. 6(a)]. The existence of a substrate band edge will have an effect on the surface energy in two ways. First, the energy-dependent phase shift for the wave-function reflection at a metal-insulator interface exhibits a van Hove-like $\sqrt{(E - E_0)}$ singularity near the semiconductor band edge and is approximately constant below E_0 . Therefore, the variation of the QWS energy as a function of film thickness in a given branch will exhibit a kink across the band edge.

Second, and more importantly, the QWS near the band edge exhibits a significant change in the in-plane effective mass, as

observed by angle-resolved photoemission experiments.^{34,35} The measured results could be an order of magnitude larger than the bulk value and could even have a sign change.³⁴ This anomalous mass enhancement is absent for deeper-lying QWSs. Since the calculation of the surface energy needs to sum up all occupied bands, the significant change in the in-plane effective mass of the QWS near the band edge will modify the final oscillation pattern of the surface energy. In contrast, the work function variation is determined by the QWS near the Fermi level. Whenever a QWS channel passes through E_F as the thickness is varied continuously, a strong dip in the work function occurs. Only the states near the Fermi level are relevant for this case; therefore, the oscillation in the work function is little affected by the existence of a substrate band edge. On the other hand, when a QWS gets close and crosses the substrate band edge, the behavior of the surface energy variation is modified. The experimental finding of a lack of the anticipated quarter phase difference between the oscillations of the surface energy and the work function in Pb/Si(111) indicates that the substrate band edge plays an important role in determining the quantum oscillation patterns in these films.

We provide further experimental evidences for the influence of the substrate band edge on the behavior of QWS. In our STS studies of the QWS energy [Fig. 2(e)], if one traces the variation of individual QWS branches as a function of the layer thickness (connected by the solid line), instead of a smooth variation, often a kink is observed somewhere between 0.4 to 0.8 eV above E_F (highlighted by the gray shade), which coincides with the position of the conduction band minimum (CBM) of the underlying Si. This is more clearly shown in Fig. 6(b), where the first derivative of QWS energy is plotted as a function of the QWS energy. Near the CBM, distinctive kinks are present for the second to eighth QWS branches. Even though the number of data points is not large enough to allow us to directly identify the location of the kink in the variation of

QWS energy of filled states, one can expect similar phenomena observed in empty states. In fact, in a recent angle-resolved photoemission spectroscopy (ARPES) study of epitaxial Pb on Ge(111), we noted that Tang *et al.*³⁶ reported that the variation of filled-state QWS energy as a function of thickness exhibits a kink when it crosses the valence band maximum (VBM) (about 0.4 eV below E_F). Similar behavior should be expected, given that in an earlier ARPES study of Pb on Si(111), it was found that E_F was pinned at a similar location above the VBM.^{34,35} Thus, experimental evidences (based on our STS data and others' ARPES studies) for the variation of QWS energy in each branch support our conjecture that the band edges of the substrate play a critical role in determining the phase of the quantum oscillations of surface energy.

V. SUMMARY

In summary, we have experimentally investigated the phase relationship of the quantum oscillations phenomena of surface energy and work function (i.e., E_s vs L and W vs L) in Pb thin films on Si(111). Contrary to a quarter wavelength phase shift predicted theoretically, we found that there is no phase shift relationship. We further proposed a conjecture to resolve this apparent inconsistency by arguing that this phenomenon is related to the critical roles that the substrate band edges play in the quantum size effect of the surface energy. We also argue that the anomalous lateral mass enhancement for QWS near the E_F , reported earlier, is due to a similar manifestation of the band edge on the quantum confinements of electronic states in ultrathin Pb films.

ACKNOWLEDGMENTS

This work was supported by National Science Foundation Grants No. DMR-0906025, CMMI-0928664, and Welch Foundation F-1672. M.-Y.C. acknowledges support by Department of Energy Grant DE-FG02-97ER45632.

*Present address: Department of Physics, University of Ulsan, Ulsan 680-749, Republic of Korea.

†Corresponding author: shih@physics.utexas.edu

¹B. J. Hinch, C. Koziol, J. P. Toennies, and G. Zhang, *Europhys. Lett.* **10**, 341 (1989).

²A. R. Smith, K. J. Chao, Q. Niu, and C. K. Shih, *Science* **273**, 226 (1996).

³Z. Y. Zhang, Q. Niu, and C. K. Shih, *Phys. Rev. Lett.* **80**, 5381 (1998).

⁴L. Huang, S. J. Chey, and J. H. Weaver, *Surf. Sci.* **416**, L1101 (1998).

⁵M. Hupalo, V. Yeh, L. Berbil-Bautista, S. Kremmer, E. Abram, and M. C. Tringides, *Phys. Rev. B* **64**, 155307 (2001).

⁶W. B. Su, S. H. Chang, W. B. Jian, C. S. Chang, L. J. Chen, and T. T. Tsong, *Phys. Rev. Lett.* **86**, 5116 (2001).

⁷S. H. Chang, W. B. Su, W. B. Jian, C. S. Chang, L. J. Chen, and T. T. Tsong, *Phys. Rev. B* **65**, 245401 (2002).

⁸H. Liu, Y. F. Zhang, D. Y. Wang, M. H. Pan, J. F. Jia, and Q. K. Xue, *Surf. Sci.* **571**, 5 (2004).

⁹M. M. Ozer, Y. Jia, B. Wu, Z. Y. Zhang, and H. H. Weitering, *Phys. Rev. B* **72**, 113409 (2005).

¹⁰M. H. Upton, C. M. Wei, M. Y. Chou, T. Miller, and T. C. Chiang, *Phys. Rev. Lett.* **93**, 026802 (2004).

¹¹R. Otero, A. L. Vazquez de Parga, and R. Miranda, *Phys. Rev. B* **66**, 115401 (2002).

¹²G. Materzanini, P. Saalfrank, and P. J. D. Lindan, *Phys. Rev. B* **63**, 235405 (2001).

¹³E. Ogando, N. Zabala, E. V. Chulkov, and M. J. Puska, *Phys. Rev. B* **69**, 153410 (2004).

¹⁴F. K. Schulte, *Surf. Sci.* **55**, 427 (1976).

¹⁵J. J. Paggel, C. M. Wei, M. Y. Chou, D. A. Luh, T. Miller, and T. C. Chiang, *Phys. Rev. B* **66**, 233403 (2002).

¹⁶Y. Qi, X. Ma, P. Jiang, S. H. Ji, Y. S. Fu, J. F. Jia, Q. K. Xue, and S. B. Zhang, *Appl. Phys. Lett.* **90**, 013109 (2007).

¹⁷X. C. Ma, P. Jiang, Y. Qi, J. F. Jia, Y. Yang, W. H. Duan, W. X. Li, X. Bao, S. B. Zhang, and Q. K. Xue, *Proc. Natl. Acad. Sci. USA* **104**, 9204 (2007).

- ¹⁸P. S. Kirchmann, M. Wolf, J. H. Dil, K. Horn, and U. Bovensiepen, *Phys. Rev. B* **76**, 075406 (2007).
- ¹⁹J. Kim, S. Y. Qin, W. Yao, Q. Niu, M. Y. Chou, and C. K. Shih, *Proc. Natl. Acad. Sci. USA* **107**, 12761 (2010).
- ²⁰C. M. Wei and M. Y. Chou, *Phys. Rev. B* **66**, 233408 (2002).
- ²¹Y. Jia, B. Wu, H. H. Weitering, and Z. Y. Zhang, *Phys. Rev. B* **74**, 035433 (2006).
- ²²T. Miller, M. Y. Chou, and T. C. Chiang, *Phys. Rev. Lett.* **102**, 236803 (2009).
- ²³D. A. Luh, T. Miller, J. J. Paggel, M. Y. Chou, and T. C. Chiang, *Science* **292**, 1131 (2001).
- ²⁴I. B. Altfeder, K. A. Matveev, and D. M. Chen, *Phys. Rev. Lett.* **78**, 2815 (1997).
- ²⁵H. Okamoto, D. M. Chen, and T. Yamada, *Phys. Rev. Lett.* **89**, 256101 (2002).
- ²⁶C. S. Jiang, S. C. Li, H. B. Yu, D. Eom, X. D. Wang, P. Ebert, J. F. Jia, Q. K. Xue, and C. K. Shih, *Phys. Rev. Lett.* **92**, 106104 (2004).
- ²⁷S. C. Li, X. C. Ma, J. F. Jia, Y. F. Zhang, D. M. Chen, Q. Niu, F. Liu, P. S. Weiss, and Q. K. Xue, *Phys. Rev. B* **74**, 075410 (2006).
- ²⁸I. Horcas, R. Fernandez, J. M. Gomez-Rodriguez, J. Colchero, J. Gomez-Herrero, and A. M. Baro, *Rev. Sci. Instrum.* **78**, 013705 (2007).
- ²⁹M. Hupalo and M. C. Tringides, *Phys. Rev. B* **65**, 115406 (2002).
- ³⁰P. Czoschke, H. W. Hong, L. Basile, and T. C. Chiang, *Phys. Rev. Lett.* **93**, 036103 (2004).
- ³¹P. Czoschke, H. Hong, L. Basile, and T. C. Chiang, *Phys. Rev. B* **72**, 075402 (2005).
- ³²T. A. Witten and L. M. Sander, *Phys. Rev. Lett.* **47**, 1400 (1981).
- ³³S. M. Binz, M. Hupalo, and M. C. Tringides, *Phys. Rev. B* **78**, 193407 (2008).
- ³⁴M. H. Upton, T. Miller, and T. C. Chiang, *Phys. Rev. B* **71**, 033403 (2005).
- ³⁵J. H. Dil, J. W. Kim, T. Kampen, K. Horn, and A. R. H. F. Ettema, *Phys. Rev. B* **73**, 161308(R) (2006).
- ³⁶S. J. Tang, C. Y. Lee, C. C. Huang, T. R. Chang, C. M. Cheng, K. D. Tsuei, H. T. Jeng, V. Yeh, and T. C. Chiang, *Phys. Rev. Lett.* **107**, 066802 (2011).